Numerical Simulation of the Supersonic Flow over Forward-Facing Step in Micro Couette Flow Using Direct Simulation Monte Carlo Method

S. Sattari*
Department of Mechanical Engineering,
Babol University of Technology, Iran
E-mail: Sajjad.Sattari@gmail.com
*Corresponding author

M. Jahani & M. Gorji-Bandpy
Department of Mechanical Engineering,
Babol University of Technology, Iran
E-mail: Mahsa.jahani89@yahoo.com, gorji@nit.ac.ir

Received: 13 March 2015, Revised: 11 July 2015, Accepted: 9 July 2015

Abstract: This work deals with a numerical study on forward-facing steps situated in a supersonic flow. The primary aim of this paper is to examine the sensitivity of the velocity, density, pressure and temperature due to the step-height variations of such forward-facing steps. Effects on the flowfield structure due to variations on the step height have been investigated by employing the Direct Simulation Monte Carlo (DSMC) method. The studied parameter contours for various values of step heights and profiles in three different sections of the channel are obtained. The results indicate that the fluid flow and temperature characteristics considerably depend on the step heights. The results were also compared with the previously published works which approved outstanding validation.

Keywords: DSMC, Supersonic Flow, Rarefied Flow, Forward-Facing Step, Micro Couette Flow

Reference: Sattari, S., Jahani, M., Gorji-Bandpy, M., "Numerical Simulation of the Supersonic Flow over Forward-Facing Step in Micro Couette Flow Using Direct Simulation Monte Carlo Method", Int J of Advanced Design and Manufacturing Technology, Vol. 8/ No. 3, 2015, pp. 49-57.

Biographical notes: S. Sattari is currently MSc student in Mechanical Engineering in Islamic Azad University of Najafabad (IAUN), Iran. He received his BSc in Mechanical Engineering from Babol University of Technology, Iran. **M. Jahani** is currently MSc student in Mechanical Engineering in Isfahan University, Iran. She received his BSc in Mechanical Engineering from Babol University of Technology, Iran. **M. Gorji-Bandpy** is currently Full Professor at the department of Mechanical Engineering, Babol University of Technology, Babol, Iran.

1 INTRODUCTION

Experimental and numerical investigations of micro and nano scale flows have drawn much attention over the last few years. Most of the areas of interest are related to microchannels, micropumps, and micronozzles, with their subsequent applications to propulsion devices, chemical and pressure sensors [1]. A channel with forward-facing step is an important geometry that is a common integral part of many micromechanical devices. The goal of this work is the numerical modeling of flows in microchannels aimed at studying the fluid flow and heat transfer in supersonic flows. The study of flows through microchannels with forward and backward-facing step has been discussed by a number of researchers.

The flow over backward-facing steps, through a grooved channel and into a cavity has been studied before [2]. Pressure and mass flow rates have been measured through microchannel devices with contraction and expansion sections, as in ref. [3]. The rarefaction and compressibility effects in microflows emphasizing that both need to be considered if one is to correctly model the physics of micro flows has been discussed [4]. Although the specific configurations of the microchannel devices differ among these researchers, the flows share common features in that they are subsonic, of relatively low Reynolds number, and have a Knudsen number in the slip-flow regime (typically between 0.01 and 0.05).

It was recognized that due to the finite Knudsen number, the flow field macroparameters, such as, pressure, temperature, and mass flow rate, could not be calculated with the standard continuum, Navier-Stokes equations. In terms of kinetic approaches, analytic formulas for the free molecular regime are not generally applicable either. However, the Navier-Stokes equations may be used with reasonable accuracy if the surface velocity-slip condition are appropriately modified [3-5]. Direct Simulation Monte Carlo (DSMC) method is rigorous because the gas-surface interaction is modeled without approximation. For this reason, DSMC calculations were performed, for selected microchannel configurations, but the primary emphasis of these calculations was to validate slip-flow correction models rather than to use DSMC as a simulation tool to study physics of the flow.

The analytic expressions for mass flow rate and pressure that include rarefaction effects such as velocity and temperature jump conditions at the gas-wall boundary and compressibility effects have been used to interpret full numerical simulation as well as experimental data, as in ref. [3-6]. Laminar hypersonic flow over forward and backward-facing steps by employing Navier-Stokes equations has been investigated in ref. [7]. The hypersonic flows over the steps were simulated by considering freestream Mach Number of 8, and Reynolds number of 108. A numerical study on backward-facing steps, situated in a rarefied hypersonic flow, has been examined by using the DSMC method, as in ref. [8]. The work was motivated by the interest in investigating the step height effects on the flow field structure. The primary emphasis was to examine the sensitivity of velocity, density, pressure and temperature fields with respect to step height variations of such backward-facing steps. In doing so, the Direct Simulation Monte Carlo (DSMC) method has been employed to calculate the supersonic two-dimensional flow over the steps.

2 GEOMETRY DEFINITION

Fig. 1 illustrates a schematic view of the studied model. According to that figure, the Mach number at infinite (M_∞) represents the upper wall velocity Mach number, and $u_{(w)}$, h , H, L are upper wall velocity, step height and channel height and total length of the channel, respectively. D stands for the location of the step. It is assumed that the channel is infinitely long thus only length L is considered. In this study the values of $h=2\times10^{-7}$, 3×10^{-7}, 4×10^{-7}m, $H=6\times10^{-7}$m, $D=2.03\times10^{6}$m and $L=6\times\times10^{-6}$m are assumed for the investigation.

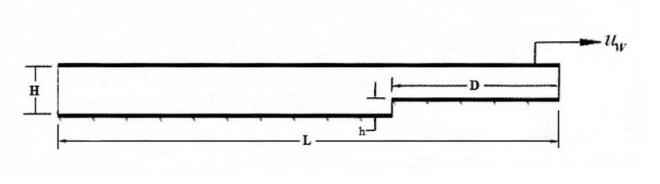

Fig. 1 Schematic diagram of the forward-facing step

An understanding of the step height effect on the aerodynamic surface properties can be obtained by comparing the flowfield behaviour of micro Couette flow with and without a step. Therefore in this study, a micro Couette flow without step is considered as a benchmark.

3 COMPUTATIONAL METHOD AND PROCEDURE

The degree of departure of a flow from continuum is indicated by the flow Knudsen number, = λ /l ; where λ and l are molecular mean free path and characteristic length of the flow, respectively. Traditionally, flows are divided into four regimes Kn<0.01, continuum flow regime, 0.01<Kn<0.1, slip flow regime, 0.1<Kn<10, transition flow regime, and Kn>10, free molecular flow regime or collisionless flow regime [9]. Based on these

flow regimes, the choice of the numerical approach to be used to model the rarefied flows, greatly relies on the extent of flow rarefaction. For near continuum flows, it is usually sufficient to take into account the effects of rarefaction through the boundary condition of slip velocity and temperature jump on the surface.

The Navier-Stokes equations, commonly used with these boundary conditions, can be delivered from the Boltzmann equation under the assumption of small deviation of the distribution function from equilibrium. Nevertheless, the Navier-Stokes equations became unsuitable for studying rarefied flows where the distribution function becomes considerable in non-equilibrium.

In order to study the flow, DSMC method is usually employed [10]. This method has become the most computational technique for modeling complex flows of engineering interest. The DSMC method simulates real gas flows with various physical processes by using a computer to track the trajectory of simulated particles, where each simulated particles represents a fixed number of real gas particles. The simulated particles are allowed to move and collide, while the computer stores their position coordinates, velocities and other physical properties such as internal energy.

The particle evolution is divided into two independent phases and the collision phases. In the movement phase, all particles are moved over distances appropriate to a short time interval. The particles that strike the solid wall would reflect according to the appropriate gas-surface interaction models. These models include specular, diffuse or a combination of these. In the collision phase, intermolecular collisions are performed according to the theory of probability without time being consumed. In this way, the intermolecular collisions are uncoupled to the translational molecular motion over the time step used to advance the simulation. The simulation is always calculated as unsteady flow; however, a steady flow solution is obtained as the large time state of the simulation.

The numerical accuracy in DSMC method depends on the cell size chosen, the time step and the number of particles per computational cell. In the DSMC code, the linear dimensions of the cells should be small in comparison with the scale length of the macroscopic flow gradients normal to the streamwise directions, which means that the cell dimensions should be in the order of or smaller than the local mean free path [11]. The time step should be chosen to be sufficiently small in comparison to the local mean collision time [12],[13]. In general, the total simulation time, discretized into time step, is based on the physical time of the real flow.

Finally, the number of simulated particles has to be large enough to make statistical correlation between particles significant [13], [14]. These effects were investigated in order to determine the number of cells and number of particles required to achieve grid independent solutions. Grid dependency was tested by running the calculations with double the number of cells in the coordinated directions compared to a standard grid (Fig. 2 and Fig. 3).

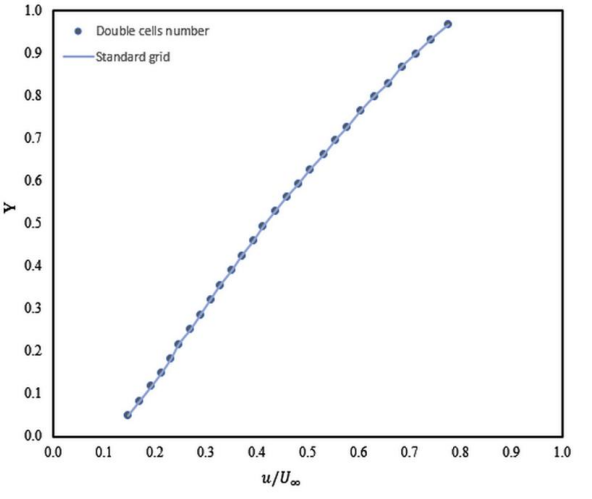

Fig. 2 Grid dependency for Couette flow at distance X=0.33

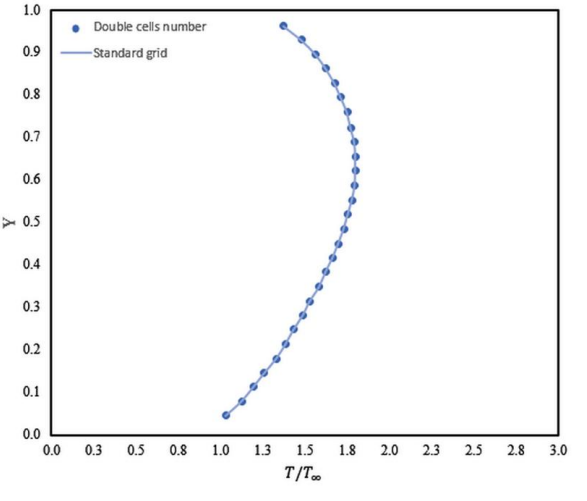

Fig. 3 Grid dependency for Couette flow at distance X=0.33

In the present account, the molecular collision kinetics is modeled by using the Variable Hard Sphere (VHS) molecular model and the No Time Counter (NTC) collision sampling technique [16], [17]. The VHS model employ the simple hard sphere angular scattering law so that all directions are equally possible for post-collision velocity in the center of mass frame of reference. Nevertheless, the collision cross section depends on the relative velocity of colliding molecules.

The mechanics of the energy exchange processes between kinetic and internal modes for rotation are controlled by the Borgnakke-Larsen statistical model [18]. Simulations are performed using gas model, consisting of N_2.

4 BOUNDARY CONDITIONS

In this study, T_∞, P_∞, ρ_∞, μ_∞, n_∞, λ_∞ and u_w stand for temperature, pressure, density, viscosity, number density, molecular mean free path and upper wall velocity, respectively. m, d and ω are molecular mass, molecular diameter and viscosity index. The upper plate velocity u_w, assumed to be constant at 1465.225 m/s, corresponds to a Mach number. M_∞ of 4.15 and the walls temperature T_w are assumed constant at 323K. It is important to mention that the surface temperature is low compared to the stagnation temperature of the N_2. This assumption seems reasonable since practical surface materials will probably be destroyed if surface temperature is allowed to approach the stagnation temperature. Finally, the Knudsen number Kn and Re corresponds to channel height are 0.062 and 56.6, respectively.

5 COMPUTATIONAL RESULTS AND DISCUSSION

5.1. Velocity field

In the DSMC method, the macroscopic properties are computed as averages from the microscopic properties of the molecules in each cell in the computational domain. In this way, the velocity is given as :

$$c_o = \frac{\sum_{j=1}^{N} (mc)_j}{\sum_{j=1}^{N} m_j} \tag{1}$$

Where N, m and c represent number of molecules, mass and velocity vector of the molecules in each cell, respectively. It should be noted that the mean molecules velocity defines the macroscopic mean velocity. It is important to mention that the velocity of the molecules relative to the mean macroscopic velocity, defined as thermal or peculiar velocity, is denoted by $c' \equiv c - c_o$. The distribution of tangential velocity u/U_∞ for three distances (X=0.16, 0.33 and 0.56) along the surface is illustrated in Figs. 4, 5 and 6 for different value of height h. In these figures, X represent the distance x normalized by the L, and Y the distance y normalized by H.

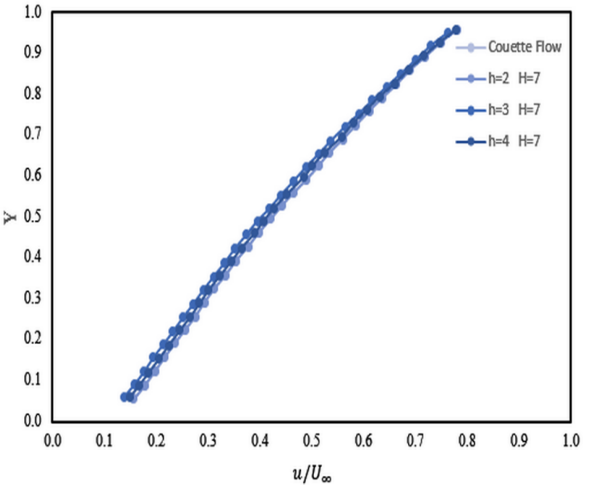

Fig. 4 Distribution of tangential velocity u/U_∞ profiles along the surface of the forward-facing as a function of the step height h for $x = 0.16$

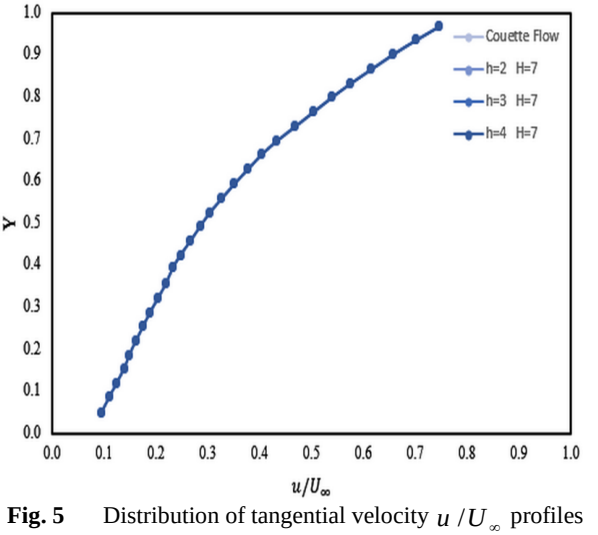

Fig. 5 Distribution of tangential velocity u/U_∞ profiles along the surface of the forward-facing as a function of the step height h for $x = 0.33$

The distribution of tangential velocity along the upstream of the step is displayed in Fig. 6 for forward-facing step at $x = 0.35$. It is observed that the velocity profiles is similar to Couette flow at the upstream of the micro channel while it deviates from the Couette flow profile at the vicinity of the step as step height h increases. In addition, the magnitude of velocity becomes negative for $h = 3\times10^{-7}$ and 4×10^{-7} indicating a recirculation region. It is clearly seen that $u/U_\infty \neq 0$ for $u/U_\infty \approx 0$, a characteristic of a rarefied flow. As a result, the condition of $u/U_\infty = 0$ at the body surface no-slip velocity in the continuum flow

regime, is not applied in rarefied flow. In order to emphasize important features in the flowfield structure, streamlines at the vicinity of the steps are demonstrated in Fig. 7-Fig. 9; it is clear that the flowfield experiences a contraction around the corner of the step and forms a recirculation region at the front face of the steps. It is also observed that the recirculation region slightly increases with increase in the front face height H.

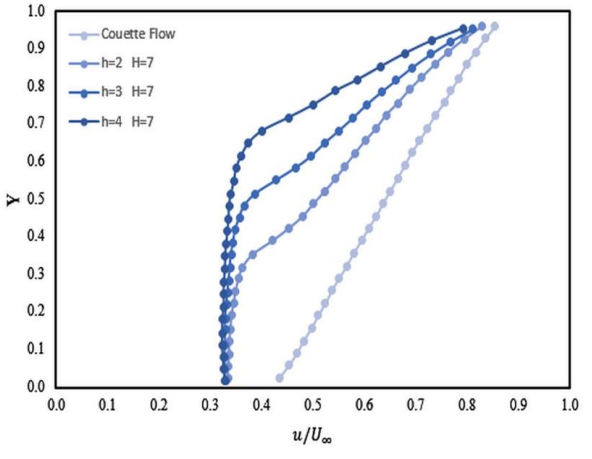

Fig. 6 Distribution of tangential velocity u/U_∞ profiles along the surface of the forward-facing as a function of the step height h for $x = 0.65$

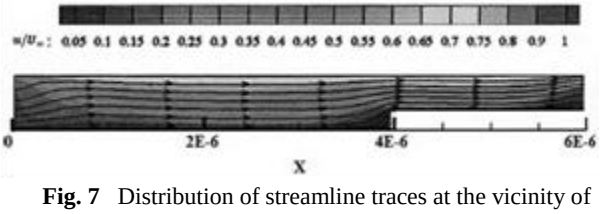

Fig. 7 Distribution of streamline traces at the vicinity of the forward-facing step with step height h for $h = 2\times10^{-7}$

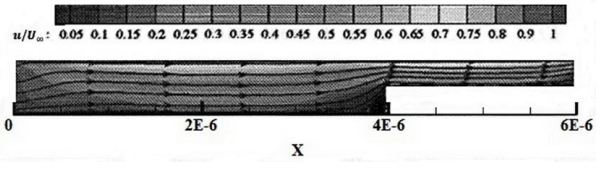

Fig. 8 Distribution of streamline traces at the vicinity of the forward-facing step with step height h for $h = 3\times10^{-7}$

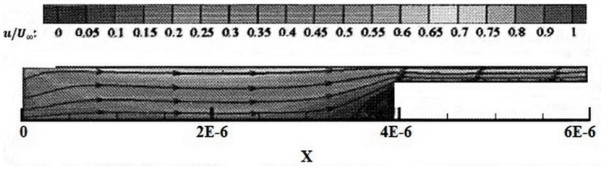

Fig. 9 Distribution of streamline traces at the vicinity of the forward-facing step with step height h for $h = 4\times10^{-7}$

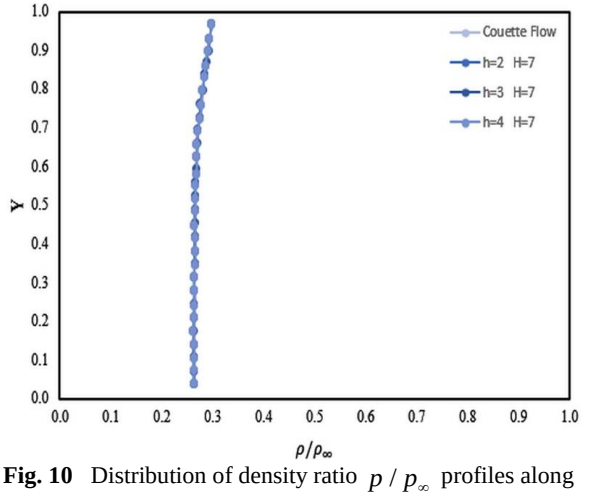

Fig. 10 Distribution of density ratio p/p_∞ profiles along the surface of the forward-facing as a function of the step height h for $x = 0.16$

5.2. Density field

The density in each cell in the computational domain is obtained by the following,

$$\rho = \frac{1}{V_c}\sum_{j=1}^{N} m_j \tag{2}$$

Where N is the number of molecules in the cell, m is the mass of the molecules and V_c is the volume of the cell, respectively. The distribution of density profiles ρ/ρ_∞ for three distance along the surface are displayed in Figs. 10, 11 and 12 for various values of h. Similar to the distribution of tangential velocity, the distribution of density profiles is shown for X=0.16, 0.33 and 0.65. X represent the distance x normalized by the L and Y the distance y normalized by H; it may be recognized from this figure that density profiles are affected due to the presence of the step.

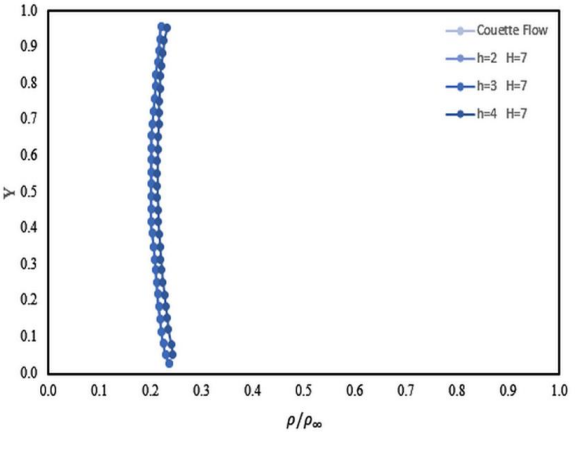

Fig. 11 Distribution of density ratio p/p_∞ profiles along the surface of the forward-facing as a function of the step height h for $x = 0.33$

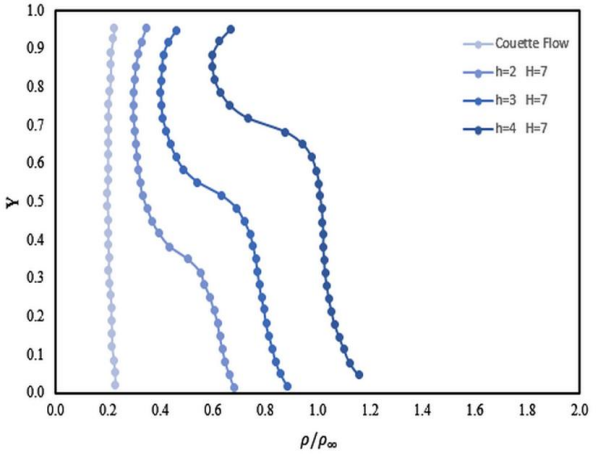

Fig. 12 Distribution of density ratio p / p_∞ profiles along the surface of the forward-facing as a function of the step height h for $x = 0.65$

As expected, at the upstream density ρ dramatically increases as compared to the inlet density ρ_∞ at the vicinity of the front step for X=0.65. It is also seen that, far from the step, the density profiles seem to approach the Couette flow density profile. In Fig. 13-Fig. 15 density ratio contours at the vicinity of the steps are displayed. The density value increases along the channel before the rare face of the step. Moreover as h increases the maximum value of normalized density also increases from 1.3 to 1.5.

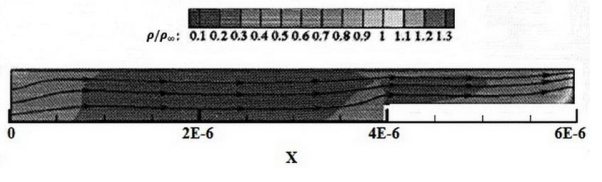

Fig. 13 Density ratio p / p_∞ contours at the vicinity of the forward-facing step with step height h for (a) $h = 2\times10^{-7}$

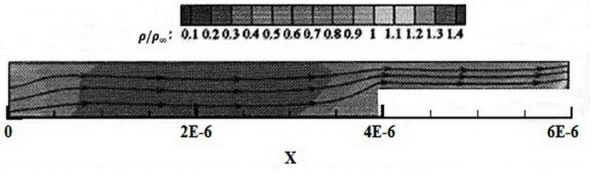

Fig. 14 Density ratio p / p_∞ contours at the vicinity of the forward-facing step with step height h for (a) $h = 3\times10^{-7}$

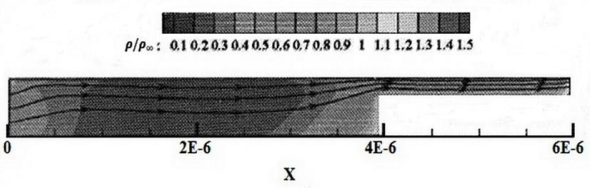

Fig. 15 Density ratio p / p_∞ contours at the vicinity of the forward-facing step with step height h for (a) $h = 4\times10^{-7}$

5.3. Pressure field

The pressure in each cell inside the computational domain is obtained by the following equation :

$$P = \frac{1}{3V_c}\sum_{j=1}^{N}\frac{\left(mc^2\right)_j}{N} \tag{3}$$

Where N is the number of molecules in the cell, m is the mass of molecules and V_c is the volume of the cell and c is the velocity of the molecules. The distribution of the pressure P/P_∞ for X=0.16, 0.33 and 0.65 along the surface is illustrated in Fig. 16-Fig. 18 for various values of h. X represent the distance x normalized by the L and Y the distance y normalized by H. As shown the pressure profiles follow a similar behavior as those for density. The value of pressure increases in the perpendicular direction for X=0.16 as seen in Fig. 16 and Fig. 17. For X=0.33 the pressure variation along the perpendicular direction is negligible while the figures shows it reaches its maximum value at the center of the channel when we approach the rate face of the step. The Fig. 18 indicates that for X=0.65 as h enhanced the peak of the pressure profiles moves toward the top surface of the channel.

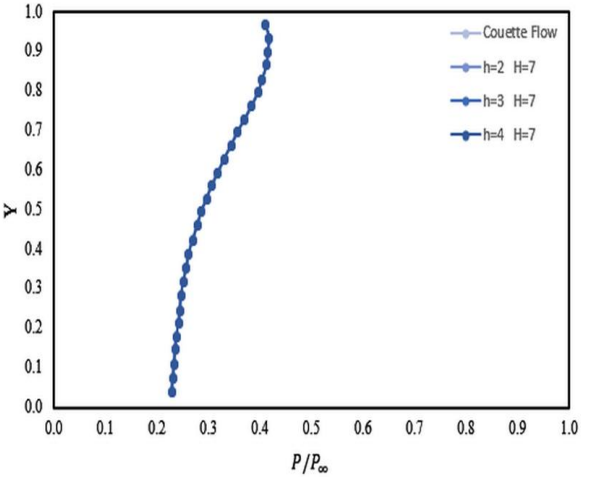

Fig. 16 Distribution Pressure ratio p / p_∞ profiles along the surface of the forward-facing as a function of the step height h for $x = 0.16$

Fig. 19-Fig. 21 illustrate the normalized pressure contour P/P_∞ in the channel. The pressure value increases along the channel before the rare face of the step, then decreases gradually; afterward the pressure reaches to its maximum value at the end of the channel. The figures also show that increases of h leads the pressure enhances above the step.

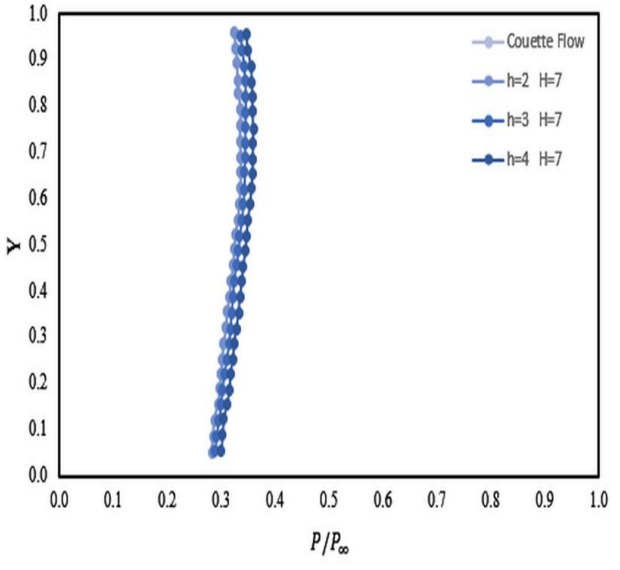

Fig. 17 Distribution Pressure ratio p/p_∞ profiles along the surface of the forward-facing as a function of the step height h for (b) $x = 0.33$

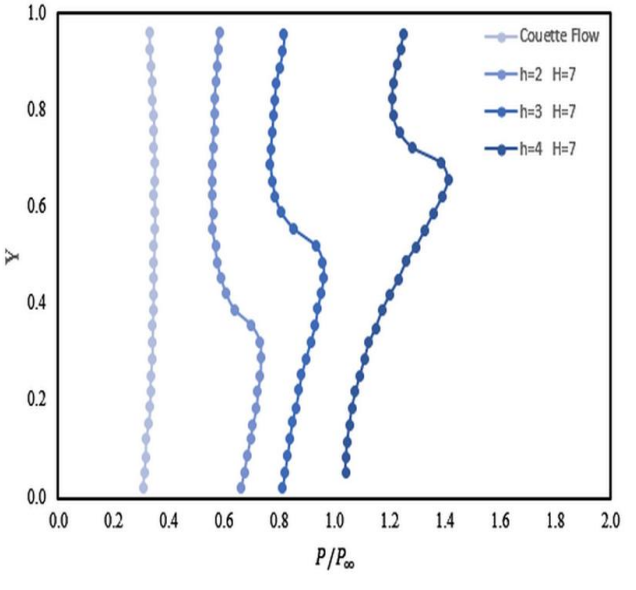

Fig. 18 Distribution Pressure ratio p/p_∞ profiles along the surface of the forward-facing as a function of the step height h for $x = 0.65$

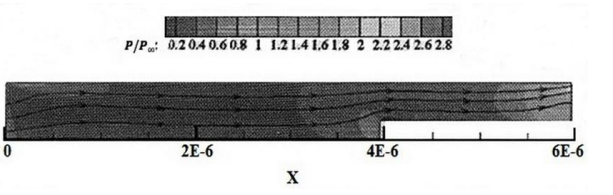

Fig. 19 Pressure ratio p/p_∞ contours at the vicinity of the forward-facing step with step height h for $h = 2\times10^{-7}$

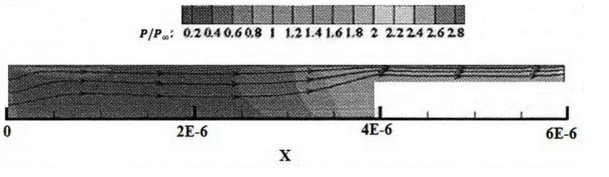

Fig. 20 Pressure ratio p/p_∞ contours at the vicinity of the forward-facing step with step height h for $h = 3\times10^{-7}$

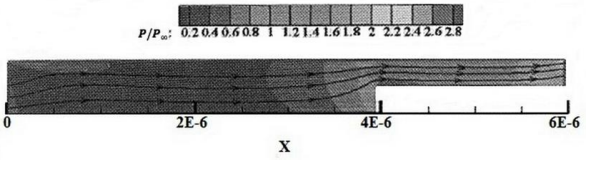

Fig. 21 Pressure ratio p/p_∞ contours at the vicinity of the forward-facing step with step height h for $h = 4\times10^{-7}$

5.4. Temperature field

The temperature in each cell inside the computational domain is obtained by the following equation,

$$T = \left(3T_{tr} + \bar{\zeta}T_{rot}\right)/\left(3+\bar{\zeta}\right) \tag{4}$$

Where T is overall temperature and T_{tr} and T_{rot} are translational and rotational temperatures, respectively. ζ is the degree of freedom. Translational and rotational temperature are define as follow,

$$T_{tr} = (\overline{mc}^{-2} - \overline{mc}_o^{\,2})/(3K/2)$$
$$T_{rot} = (2/K)(\bar{\varepsilon}_{rot}/\bar{\varsigma}) \tag{5}$$

Where K is Boltzmann constant and ε_{rot} is rotational energy of an individual molecule. Temperature ratio profiles T/T_∞ along the surface for forward-facing step are displayed in Fig. 22-Fig. 24 for X=0.16, 0.33 and 0.65. As shown, the temperature distribution is a function of the step height. Distribution of normalized

temperature profiles for various value of X is shown in Figs. 22, 23 and 24. As seen, variation of temperature distribution is similar to the pressure profile means; the temperature value increases along the channel, beside the profile deviates from the Couette flow with increases of h especially for location nearby the rare face of the step.

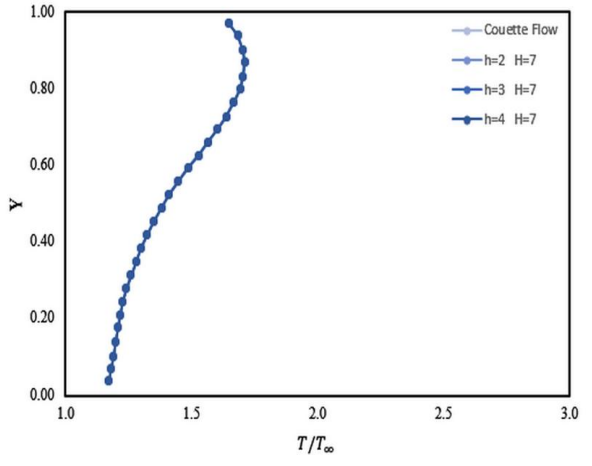

Fig. 22 Distribution Temperature ratio T/T_∞ profiles along the surface of the forward-facing as a function of the step height h for $x = 0.16$

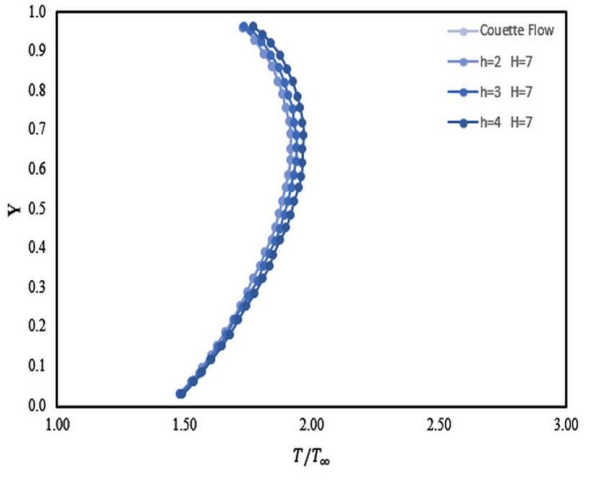

Fig. 23 Distribution Temperature ratio T/T_∞ profiles along the surface of the forward-facing as a function of the step height h for $x = 0.33$

Fig. 25-Fig. 27 show the temperature contour T/T_∞ of the channel flow for different value of step heights. As shown, there are two regions which the maximum temperature occurs; one just nearby the rare face of the step and the other at the downstream of the channel. It is worthwhile mentioning that as h increases the first region considerably develops while the region at the downstream gradually decreases.

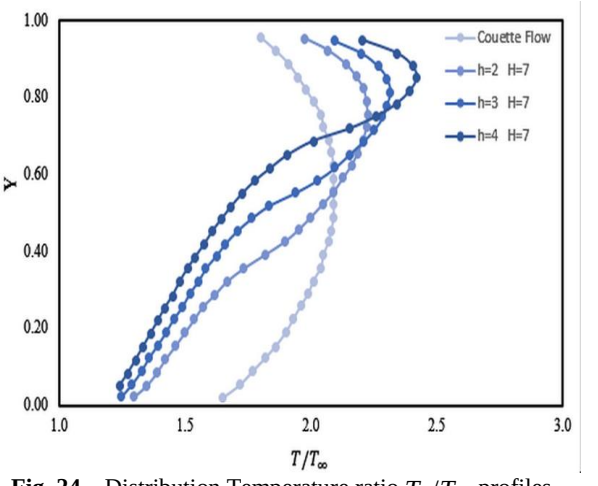

Fig. 24 Distribution Temperature ratio T/T_∞ profiles along the surface of the forward-facing as a function of the step height h for $x = 0.65$

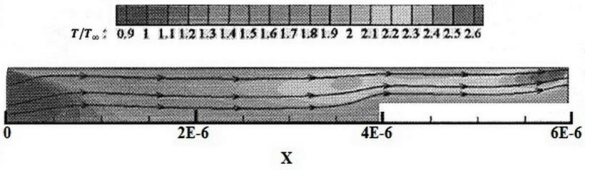

Fig. 25 Temperature ratio T/T_∞ contours at the vicinity of the forward-facing step with step height h for $h = 2\times10^{-7}$

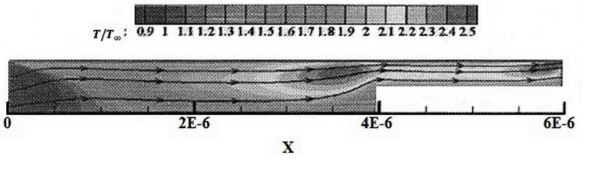

Fig. 26 . Temperature ratio (T/T_∞) contours at the vicinity of the forward-facing step with step height h for $h=3\times10^{-7}$

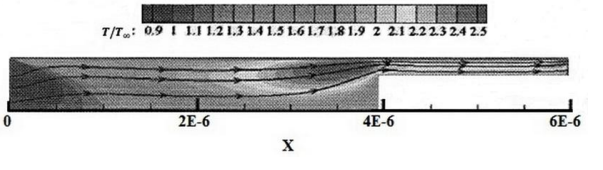

Fig. 27 Temperature ratio (T/T∞) contours at the vicinity of the forward-facing step with step height h for h=3×10-7

6 CONCLUSION

In this study, the computations of a rarefied supersonic flow on forward-facing step have been performed using the Direct Simulation Monte Carlo method. The calculation provided information concerning the nature of the flowfield structure about the primary flow properties at the vicinity of the steps. Effects of the step height on the velocity, density, pressure, and temperature for a respective range of parameters were investigated. The analysis showed that the velocity profile is similar to Couette flow at the upstream of the microchannel while it deviates from the Couette flow profile at the vicinity of the step as step height h increases. The flowfield experiences a contraction around the corner of the step and forms a recirculation region at the vicinity of the front face of the steps. In the case of temperature profiles, the maximum temperature occurs in two distinct region; one just before the rare face of the step and the other downstream of the channel.

7 REFERENCES

[1] Gad-el-Hak, M, "The fluid mechanics of microdevices", journal Fluids Engineering, Vol. 121, 1999, pp. 99-133.

[2] Karniadiakis, G. E., Beskok, A., "Micro Flows, Fundamentals and Simulation", Springer-Verlage, New York, 2002.

[3] Li, Xinxin, Lee, W. Y., Wong, M, and Zohar, Y., "Gas flows in Construction microdevices", Sensors and Actuators, Vol. 83, 2000, pp. 227-283.

[4] Beskok, A., Karniadiakis, G. E., and Trimmer, W., "Rarefaction and compressibility effects im gas microflows", Journal Fluids Engineering, Vol. 188, Sep. 1996, pp. 448-456.

[5] Lee, W. Y., Wong, M., and Zohar, Y., "Pressure loss in constriction microchannels", Journal of Microelectromechanical Systems, Vol. 11, No. 3, Jun. 2002, pp. 236-244.

[6] Arkilic, E. B., Schmidt, M. A., and Breuer, K. S., "Gaseous Slip Flow in Long Microchannels", Journal of MEMS, Vol. 6, No. 2, Jun. 1997, pp. 167-178.

[7] Grotowsky, M. G., Ballmann J., "Numerical Investigation of Hypersonic Step-Flows", Shock Waves, Vol. 10, 2000, pp. 57-72.

[8] Leite, P. H. M., Santos, W. F. N., "Direct simulation calculation of the rarefied hypersonic flow past a backward-facing step", 20th International Congress of Mechanical Engineerin, 15-20Nov. 2009, Gramado, Brazil.

[9] Schaff, S. Chambre P., "Fundamentals of gas dynamics Princeton University Press", Princeton, NJ, 1958.

[10] Bird, G. A., "Molecular gas dynamics and the direct simulation of gas flows", Oxford University Press, 1994, pp. 687-741.

[11] Alexander, F. J., Garcia, A. L., and Alder, B. J., "Erratum: Cell size dependence of transport coefficient in stochastic particle algorithms", Physics of Fluids, Vol. 12, 2000, pp. 731-731.

[12] Garcia, A. L., and Wanger, W., "Time step truncation error in Direct Simulation Monte Carlo", Physics of Fluids, Vol. 12, 2000, pp. 2621-2633.

[13] Hadjiconstantinou, N. G., "Analysis of discretization in the Direct Simulation Monte Carlo", Physics of Fluids, Vpl. 12, 2000, pp. 2634-2638.

[14] Shu, C., Mao, X. H., and Chew, Y. T., "Particle number per cell and scaling factor effect on accuracy of DSMC simulation of micro flows", Intrnational Journal of Numerical Methods for Heat and Fluid Flow, Vol. 15, No. 8, 2005, pp. 827-841.

[15] Sun, Z. X., Tang, Z., He, Y. L. and Tao, W. Q., "Proper Cell Dimension and Number of particles per cell for DSMC", Computers and Fluids, Vol. 50, 2011, pp. 1-9.

[16] Bird, G. A., "Monte Carlo Simulation in an Engineering Contaxt", Progress in Astronautics and Aeronautics: Rarefied gas Dynamics, Vol. 74, part I, AIAA, New York, 1981, pp.239-255.

[17] Bird, G. A., "Perception of Numerical Method in Rarefied Gas dynamics", Progress in Astronautics and Aeronautics, Rarefied Gas Dynamics: Theoretical and Computational Technique, Vol. 118, AAIA, New York, 1989, pp. 374-395.

[18] Borgnakke, C. Lasern, P. S., "Statistical Collision Model for Monte Carlo Simulation of Polyatomic Gas Mixture", Journal of Computational Physics, Vol. 18, No. 4, 1975, pp. 405-420.